Hindawi
Advances in Materials Science and Engineering
Volume 2022, Article ID 2713524, 9 pages
https://doi.org/10.1155/2022/2713524

Research Article

Mechanical Properties and Accuracy Evaluation of 3D Printing Based on Value in the Munsell Color System

Jianping Huang,[1] Wanxiang Ye,[2] Guihua Ye,[2] Qi Jia,[3] Kelun Li,[3] Jiawen Kong,[3] Heng Bo Jiang,[3] Qing Lan,[1] and Liming Yu[1]

[1]*Department of Stomatology, Affiliated Hospital of Guangdong Medical University, First Clinical Medical College, Guangdong Medical University, Zhanjiang, Guangdong, China*
[2]*Department of Stomatology, Dongguan Hospital of Integrated Traditional Chinese and Western Medicine, Dongguan, Guangdong, China*
[3]*The Conversationalist Club, School of Stomatology, Shandong First Medical University, Jinan, Shandong, China*

Correspondence should be addressed to Heng Bo Jiang; hengbojiang@foxmail.com and Liming Yu; 365664822@qq.com

Received 13 May 2022; Accepted 2 June 2022; Published 29 June 2022

Academic Editor: Lan Huang

Copyright © 2022 Jianping Huang et al. This is an open access article distributed under the Creative Commons Attribution License, which permits unrestricted use, distribution, and reproduction in any medium, provided the original work is properly cited.

Aim. Printing parameters have been studied extensively to improve printing performance, while resins have been studied to a lesser extent. Therefore, we explore the impact of value in the Munsell color system on the mechanical properties and accuracy of printed products. *Materials and Methods*. Resins having different values were prepared by mixing transparent resin and color pastes. We used plate models for mechanical measurement, crown-and bridge models for accuracy measurement, and disc models for color measurement. *Results*. The Group E resin, which had the lowest value, had the minimum ultimate flexural strength (61.199 MPa) and a relatively low elastic modulus (19.015 MPa). Excluding the *d* index, no significant difference in accuracy was observed. In terms of the *d* index of trueness, the result of the Group E resin was significantly low. The relative errors of trueness were less than 0.0727 μm. The relative errors of precision were less than 0.0093 μm. *Conclusion*. The value of a resin affects the mechanical properties and accuracy of printed products. It is better to secure flexural strength by using a lower-value resin. High-value resins have relatively low accuracies.

1. Introduction

Three-dimensional (3D) printing, also called additive manufacturing, refers to the fabrication of objects through the material deposition. 3D printing is widely used in aerospace, industrial, medical, and multiple other domains [1]. In dentistry, 3D printing can help reduce the time required for cumbersome tasks such as dental restoration and the fabrication of denture bases [2]. In recent years, 3D printing has evolved rapidly, and many related technologies have emerged, including vat photopolymerization, material extrusion, powder bed fusion, and material jetting. Among these 3D printing technologies, vat photopolymerization is the earliest 3D printing technique [3, 4].

Digital light processing (DLP) is a vat photopolymerization technique in which a 3D object is built in a layer-by-layer fashion through localized photopolymerization of liquid resins [5]. The DLP technique has the advantages of high printing speed and high precision of finished products. Owing to its high accuracy, this technique is used to manufacture complex or sophisticated medical devices [6].

Photocurable resins are mainly composed of a resin matrix and a photoinitiator system [7]. Photoinitiator systems usually consist of photoinitiators and coinitiators, which significantly influence the degree of conversion of photocurable dental resins. Under a light of appropriate wavelength and intensity (UV or visible light), the photoinitiator is activated, and it interacts with the coinitiator to polymerize [8]. Owing to differences in the ability of resins of different colors to absorb different light sources, the final cured product is influenced by the color of the light source used to illuminate the resin. Therefore, the use of resins of different colors may affect the quality of 3D-printed products. Lee et al. [9] used spectrophotometry to study the effect of layer thickness and printing orientation on the color of 3D printing resins. The results indicated that different layer thicknesses and print orientations significantly affect the color stability and dyeability of resins. Moreover, the degree of discoloration of a print resin varies with time. Other factors that influence the quality of 3D-printed products fabricated using the DLP technique include exposure time, wavelength of light, and amount of power supplied [5].

The Munsell color system was the first system for systematically representing the color in three dimensions. This color system allows for accurate color specification and matching in science, art, and industries by defining a coordinate system for all color perceptions [10]. The Munsell color system usually describes color through the three dimensions of value, chroma, and hue. As a standard system for color specification, it has been widely used in color science. In dentistry, the Munsell color system can be used to define the color range of natural human teeth. In recent years, several scholars have used the Munsell color system to evaluate the accuracy of tooth color or the optimal parameters of 3D printers [11, 12]. The Munsell color system has an increasingly important role in dentistry.

In the dental field, 3D-printed products with superior mechanical properties and accuracy can help with the maintenance of normal prosthesis function under the action of chewing stress [13]. In this study, we aim to combine the Munsell color system with a DLP 3D printer to explore the effect of the value dimension of color on the mechanical properties and accuracy (including trueness and precision) of 3D-printed products. The results can provide a color reference for the clinical production of restorative implants. Moreover, the results of this study can be used to identify the experimental reference conditions for color factors, which can be used in other studies, and minimize the influence of color factors on experimental results. In the experiment conducted herein, we establish two null hypotheses: the value of the resin will not affect the mechanical properties of DLP 3D-printed products, and the value of the resin will not affect the accuracy of DLP 3D-printed products.

2. Materials and Methods

2.1. Preparation of Resin. Clear resin (Basic Clear, Anycubic, China) was used as the starting material in this study. We used small amounts of black and white pigments (Black/White, Xin Jia Yi, China) to obtain black and white resins, respectively (light from the light source of the DLP printer can pass through these resins to ensure that they were not left uncured). The prepared black and white resins were mixed homogeneously in the volume ratios of 1 : 2, 1 : 1, and 2 : 1 to investigate the relationship between the color parameters and the mechanical properties and accuracy of the material in the two intervals of black and white. All mixing processes were carried out under shaded conditions with slow shaking to prevent resin denaturation and reduce bubble generation. We named the black resin and white resin with volume ratios of 0 : 1, 1 : 2, 1 : 1, 2 : 1, and 1 : 0 and the clear resin without any added pigment as A, B, C, D, E, and F, respectively, in this study, and their parameters are listed in Table 1.

2.2. CAD Design and 3D Printing. The three types of disc models (for color measurement) based on ISO-4660 [14], a plate model (for mechanical properties) based on ISO-20795-1 [15], and a crown-and-bridge model (for accuracy evaluation) based on ISO-12836 [16] were designed using AutoCAD (v.2021, Autodesk, USA), as shown in Figure 1. The five models were exported in standard tessellation language (STL) format with the highest accuracy and highest number of point clouds that the software can provide. The models were then imported into a slicing software suite (Photon Workshop v. 2.1, Anycubic, China) and sliced using a specific slice parameter by referring to the recommendations of the 3D printer manufacturer (layer thickness, 0.01 mm; normal exposure time 1.50 s; off time, 2.00 s).

The slice files were subsequently imported into the 3D printer and printed at room temperature (approximately 25°C). Six units of each of the five models were printed at the same time. The models were subjected to postprocessing immediately after printing, which included cleaning, drying, and placing the models in an ultraviolet light box for additional polymerization (crown-and-bridge model, plate model, and disc model; 10 min). The light box delivered a wavelength of 400–405 nm and a power of 15 W. Additionally, the plate models were polished using P500 and P1200 grinding papers to a thickness of approximately 3.3 mm. Photographs of the fabricated models are shown in Figure 1.

2.3. Color Measurement. According to ISO-4660, three types of disc models were printed for color measurement. (1.6 mm × 1.4 mm; 0.8 mm × 1.4 mm; 2.4 mm × 1.4 mm). These models were placed on a flat surface against matt white and black backgrounds. The models were properly aligned with the center of the color spectrophotometer's receiver (CM-26 dG, KONICA MINOLTA, JPN) to obtain accurate readings. All procedures were carried out under shaded conditions. The results were recorded using a 2° standard observer and the CIE standard illuminant D65.

2.4. Mechanical Properties. According to ISO-20795-1, we compared the ultimate flexural strength and elastic modulus of six groups of resins with those of the plate models. A universal testing machine (Z010, ZwicRoell, GER) with a constant displacement rate of 5 mm/min and a distance of 50 mm between the supports shall was used in this study. The approximate dimensions of the plate models were 60 mm × 10 mm × 3.3 mm ($N = 6$).

By referring to the data in Table 1, we selected a curve in the same group of samples as the representative curve of this group, which reflect the data in the table more intuitively. The elastic

Table 1: Groups with resins of different values.

Groups	Volume ratio of black and white resin	Value (L^*)		a^*		b^*		Transparency	Disc thickness
		White background	Black background	White background	Black background	White background	Black background		
A	0 : 1	82.95	50.67	−2.39	−2.54	10.00	−0.85	34.06	0.8
		79.46	53.37	−2.38	−3.14	11.89	0.26	28.57	1.6
		74.33	55.29	−2.21	−3.46	12.85	1.68	22.11	2.4
B	1 : 2	67.21	38.90	−0.56	−0.77	8.47	−1.13	29.90	0.8
		56.61	38.50	0.00	−0.78	7.31	−1.29	20.06	1.6
		48.85	37.37	0.30	−0.81	6.10	−0.13	13.11	2.4
C	1 : 1	63.79	36.33	−0.39	−0.23	7.69	−1.34	28.91	0.8
		53.67	34.89	0.21	−0.23	6.82	−1.59	20.58	1.6
		45.39	33.78	0.58	−0.24	5.54	−1.58	13.64	2.4
D	2 : 1	67.46	33.50	−0.67	0.11	7.49	−1.40	35.11	0.8
		51.06	31.41	0.22	0.10	7.02	−1.36	21.36	1.6
		42.47	30.12	0.71	0.26	5.00	−1.94	14.17	2.4
E	1 : 0	63.75	30.88	−0.82	0.22	7.23	−0.78	33.85	0.8
		50.21	29.36	−0.16	0.41	7.14	−1.10	22.43	1.6
		39.27	27.25	0.34	0.45	5.41	−1.05	13.65	2.4
F	Clear resin	86.93	36.27	−2.23	−0.14	8.32	−0.94	51.54	0.8
		84.44	35.62	−2.34	−0.20	10.78	−0.38	50.13	1.6
		82.48	35.85	−2.56	−0.42	11.45	0.20	48.02	2.4

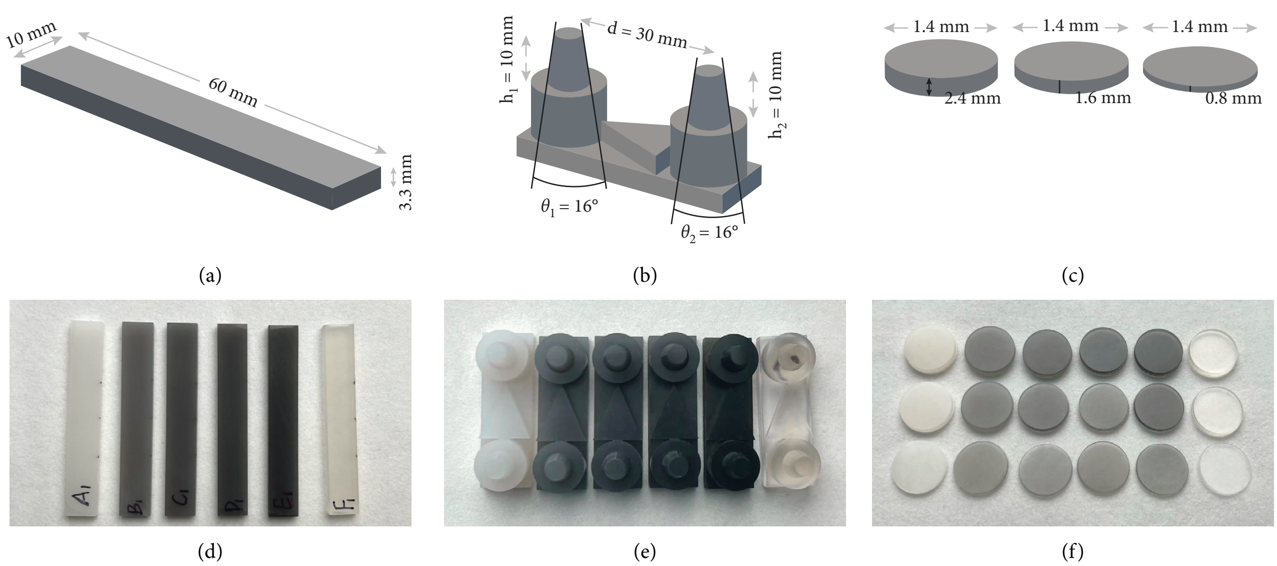

Figure 1: Schematics and actual photographs of plate model (a and d), crown-and bridge model (b and e), and disc model (c and f).

modulus was determined from the slope of the initial linear part of the strength-strain curves (Figure 2).

The ultimate flexural strength was calculated using the following equation:

$$\text{Ultimate flexural strength} = \frac{3Fl}{2wt^2}, \quad (1)$$

where F is the maximum load exerted on the specimen in Newtons; l is the distance between the supports in millimeters (50 mm in this study); w is the width of the specimen in millimeters; t is the thickness of the specimen in millimeters.

2.5. Accuracy Evaluation. According to ISO-12836, we used the crown-and-bridge models to evaluate the accuracy of printing resins of different values. A coordinate measuring machine (CMM, Axiom too CNC, Aberlink, UK) with a probe head (PH10T, Aberlink, UK) was used to measure the indexes of the models (scale resolution: 0.5 μm). The probe diameter (TP20, Standard Force, M2, Renishaw, UK) was 1 mm. The model was held tightly in a vise to prevent any change in its coordinates during measurement. All measurement processes were conducted by the same operator by manually selecting the coordinates to be measured; then, the machine automatically ran the final measurement to eliminate the effect of the strength of human measurements on the results. The planes, lines, and cones constructed during the measurement process were almost always placed at the

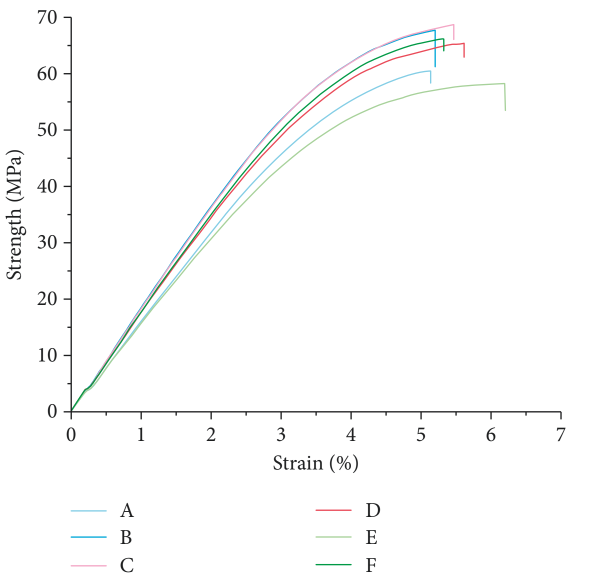

Figure 2: Strength-strain curves of resins having different values.

same position on each model to eliminate the effect of choice of measurement range on the results. Each angle of the probe was calibrated before each group of measurements. All measurement processes were conducted at 20°C, as recommended by the manufacturer. The following indexes were used: cone height (h_1, h_2), cone angle (θ_1, θ_2), and cone distance (d). The gold standard is shown in Figure 1, and its value is the same as that designed using AutoCAD ($N = 6$).

The trueness, precision, and their errors were calculated using the following equations: [17].

$$\text{Truness} = \left|(b_R - b_M)\right|, \quad (2)$$

$$\text{Precision} = \left|(b_A - b_M)\right|, \quad (3)$$

$$\Delta b_M = \left|\frac{(b_R - b_M)}{b_R}\right|, \quad (4)$$

$$\Delta S(b_M) = \left|\frac{S(b_M)}{b_R}\right|, \quad (5)$$

where b_R is the standard reference values of the indexes (height, angle, and distance) of the model (*in this study, height = 10 mm, angle = 16°, and distance = 30 mm*); b_M is the measured values of the indexes (height, angle, and distance) and angle of the model; b_A is the is the average of the measured values of the indexes (height, angle, and distance) of the model; Δb_M is the relative error of trueness; $\Delta S(b_M)$ is the relative error of precision; $S(b_M)$ is the standard deviation of measured values of the indexes (height, angle, and distance) of the model.

2.6. Statistical Analysis. All data were subjected to a one-way analysis of variance (ANOVA) and Tukey's multiple comparison post hoc test (Origin Pro 2022, Origin Lab, USA). * denotes $p < 0.05$, ** denotes $p < 0.01$, and *** denotes $p < 0.001$.

Table 2: Mean ± standard deviation of mechanical properties of resins having different values.

Groups	Ultimate flexural strength (MPa)	Elastic modulus (MPa)
A	64.274 ± 1.036	18.645 ± 0.872
B	65.786 ± 2.689	20.393 ± 0.665
C	66.054 ± 2.445	19.870 ± 0.624
D	64.320 ± 1.358	19.782 ± 0.438
E	61.199 ± 2.191	19.015 ± 0.827
F	65.118 ± 1.824	19.820 ± 0.727

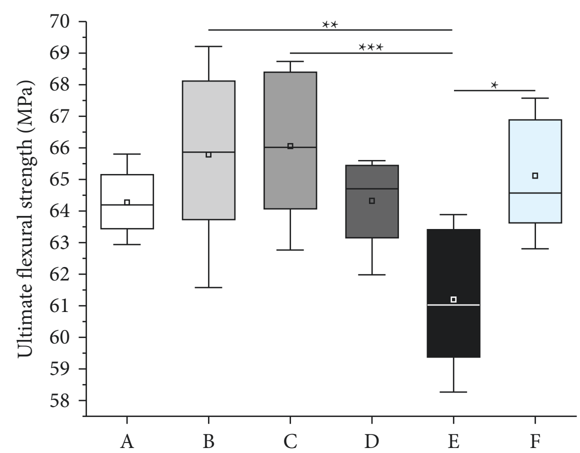

Figure 3: Ultimate flexural strength of resins having different values. $^*p < 0.05$, $^{**}p < 0.01$, and $^{***}p < 0.005$.

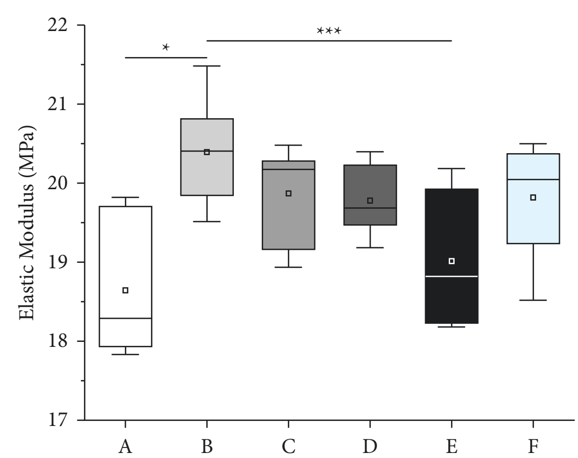

Figure 4: Elastic moduli of resins having different values. $^*p < 0.05$, $^{**}p < 0.01$, and $^{***}p < 0.005$.

3. Results

3.1. L^*, a^*, and b^* of Resins of Different Values. The L^*, a^*, and b^* values of discs of three different thicknesses and composed of resins having different values are listed in Table 2. For discs of the same thickness, as the proportion of

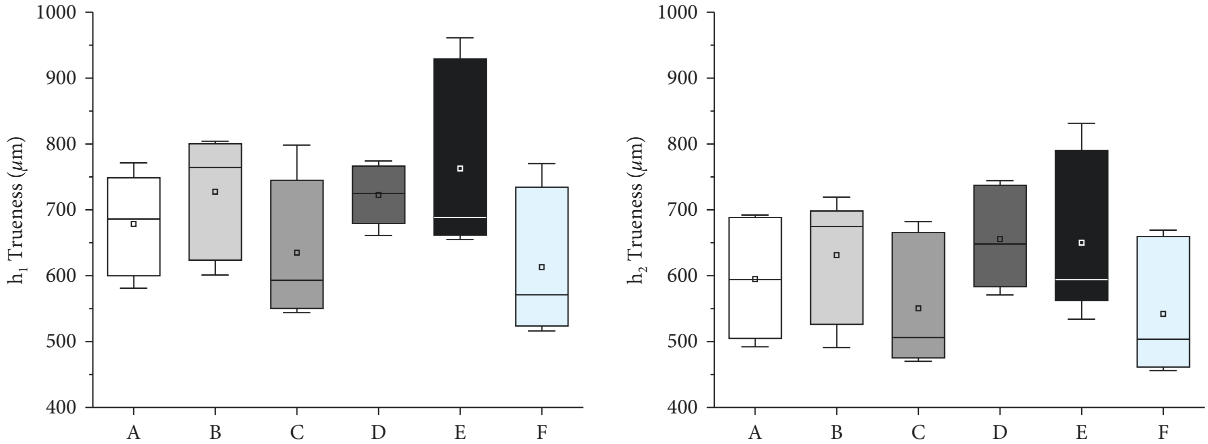

Figure 5: Boxplots of trueness for height (h).

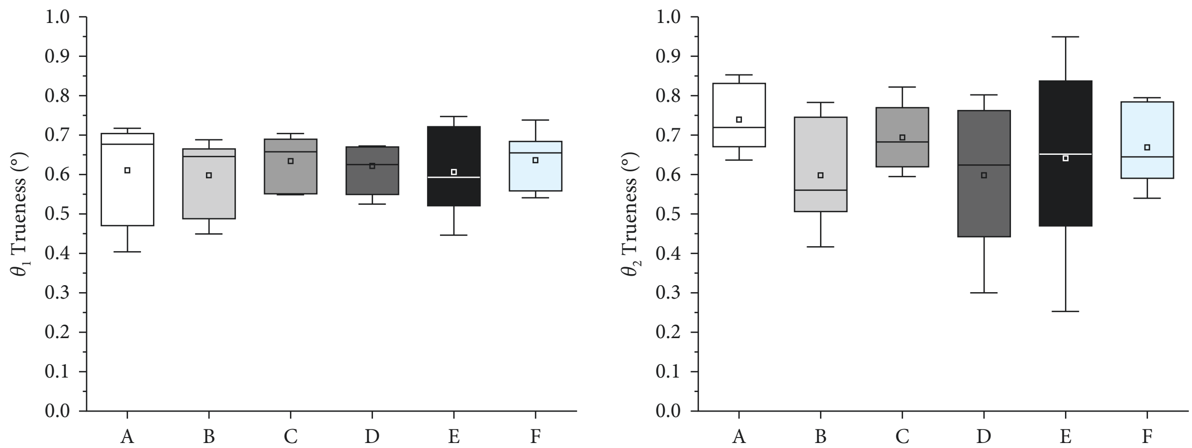

Figure 6: Boxplots of trueness for angle (θ).

black resin increased, L decreased. Except for the case of Group A on a black background, L decreased as the disc thickness increased. Based on the three-layer thicknesses, the transparency of Group A resins was higher than that of resins belonging to other groups (except Group F). The transparency of the Group F resin (clear resin) was significantly higher than those of the other groups.

3.2. Mechanical Properties of Resin of Different Values. Figure 3 and Table 2 show and summarize, respectively, the ultimate flexural strength of the six resins having different values. Except for the Group A resin, the ultimate flexural strengths of the resins belonging to the other groups decreased as their value decreased. Group E resins, which had the lowest value, had the minimum ultimate flexural strength (61.199 MPa), which was significantly lower than those of Groups B ($p < 0.01$), C ($p < 0.005$), and E ($p < 0.05$). The ultimate flexural strength of the gray resin was higher in the higher-value groups (B and C), while the ultimate flexural strength of Group A resins, which had the highest value, was less than those of Group B and C resins.

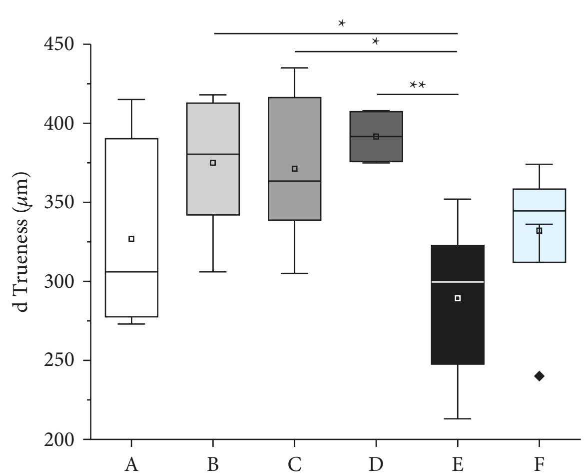

Figure 7: Boxplots of trueness for distance (d). $^{*}p < 0.05$, $^{**}p < 0.01$, $^{***}p < 0.005$.

Additionally, the ultimate flexural strength of the clear resin was relatively high, second only to those of Group B and C resins.

Table 3: Mean trueness ± standard deviation (SD) of crown-and bridge models of resins having different values.

Groups	h_1 (μm)	h_2 (μm)	θ_1 (°)	θ_2 (°)	d (μm)
A	678.500 ± 81.186	594.667 ± 91.101	0.611 ± 0.130	0.739 ± 0.087	326.833 ± 59.449
B	727.167 ± 88.984	631.333 ± 93.146	0.598 ± 0.098	0.598 ± 0.136	375.00 ± 42.019
C	634.500 ± 103.732	550.167 ± 96.013	0.634 ± 0.068	0.694 ± 0.086	371.167 ± 46.275
D	722.167 ± 50.070	655.500 ± 79.644	0.621 ± 0.064	0.598 ± 0.196	391.500 ± 14.405
E	762.500 ± 138.963	650.167 ± 122.156	0.606 ± 0.111	0.642 ± 0.238	289.333 ± 47.886
F	612.667 ± 107.224	541.833 ± 97.315	0.636 ± 0.073	0.669 ± 0.100	332.00 ± 47.079

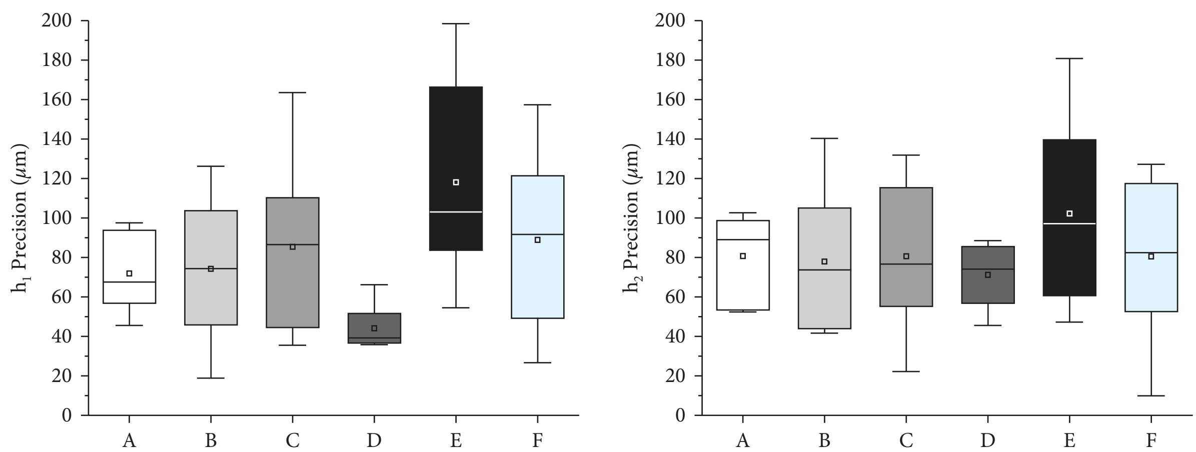

Figure 8: Boxplots of precision for height (h).

Figure 4 and Table 2 show and summarize, respectively, the elastic modulus of the six resins having different values. Similar to the results of ultimate flexural strength, the elastic modulus of the resins belonging to groups other than Group A basically decreased as their value decreased. The elastic modulus of the clear resin was relatively high, second only to those of groups B and C. The Group B resin had the highest elastic modulus (20.393 MPa), significantly higher than that of Group A (18.645 MPa, $p < 0.05$) and E (19.015 MPa, $p < 0.005$) resins. However, unlike that, Group A, with the highest value, has the lowest elastic modulus (18.645 MPa), and Group E was just above it (19.015 MPa).

3.3. Accuracy of Crown-and-Bridge Models of Different Values. Figures 5–7 and Table 3 show and summarize, respectively, the trueness of the different indexes of the crown-and-bridge model. In terms of the trueness of h and θ, there were no significant differences ($p > 0.05$). However, as for the trueness of d, the trueness of the Group E resin, which had the highest value, was significantly lower than that of Group B ($p < 0.05$), C ($p < 0.05$), and D ($p < 0.01$) resins. As summarized in Table 3, the mean trueness of d for the Group E resin was 289.333, which was the lowest and represents the best trueness. There is a deviation in the trueness value of the Group F resin, and this deviation did not affect the overall statistics.

Figures 8–10 and Table 4 show and summarize, respectively, the precision of the different indexes of the crown-and-bridge model. In terms of precision, none of the groups exhibited significant differences ($p > 0.05$). The measurements of h (118.000, 102.222) and θ (0.170) of Group E resin are highest, which is also higher in the measurement of d (35.553).

Tables 5 and 6 list the relative errors of trueness and precision. The relative errors of trueness are less than 0.0727. The relative errors of precision are less than 0.0093. Overall, the relative errors of precision are lower than those of trueness. Moreover, both types of relative errors exhibit the same trend.

4. Discussion

Based on the results of our study, the null hypothesis that value does not affect the mechanical properties and accuracy of DLP 3D-printed products was rejected. The experiment conducted herein was qualitative. The trend of each data group changed with the variables, and the pros and cons of these changes warrant attention. Moreover, the magnitude of value or the existence of a significant difference between groups may not accurately reflect the results of this study.

According to Table 1, the sample with the lowest value (Group E) has the lowest ultimate flexural strength. Additionally, the elastic modulus of the Group E resin is lower. Tahayeri et al. [18] pointed out that to deeply cure lower-value resins, higher laser intensities are required. Therefore, the curing depth of the black samples may be worse than those of the other samples under the same printing parameters and postprocessing conditions, leading to incomplete curing of black samples and easier bending and breaking. In terms of the mechanical property results, we recommend longer postcuring times for low-brightness printed products to increase the curing depth. Meanwhile,

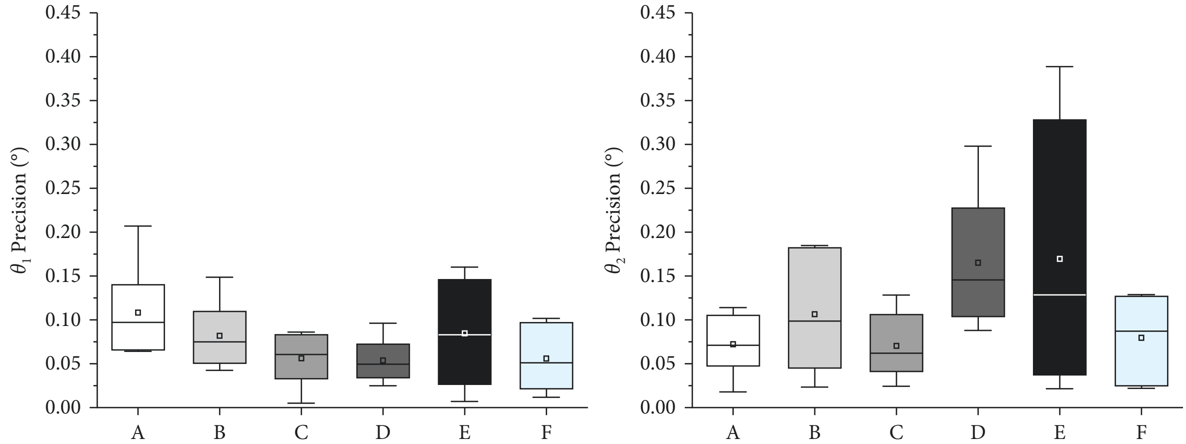

Figure 9: Boxplots of precision for angle (θ).

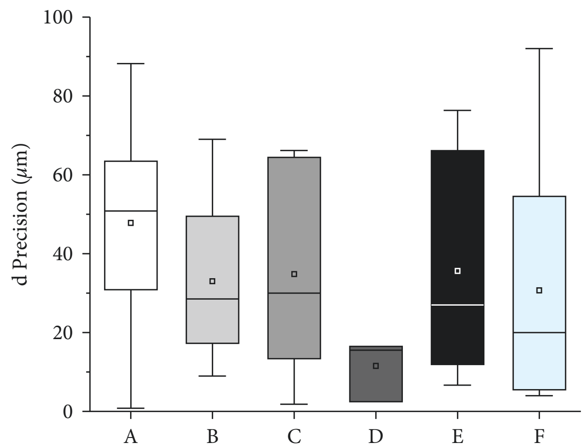

Figure 10: Boxplots of precision for distance (d).

Table 4: Mean precision ± standard deviation (SD) of the crown-and bridge models of resins having different values.

Groups	h_1 (μm)	h_2 (μm)	θ_1 (°)	θ_2 (°)	d (μm)
A	71.833 ± 19.977	80.667 ± 22.157	0.108 ± 0.053	0.072 ± 0.035	47.778 ± 28.194
B	74.111 ± 36.431	77.889 ± 37.366	0.082 ± 0.039	0.106 ± 0.070	33.000 ± 21.420
C	85.333 ± 44.969	80.556 ± 37.836	0.056 ± 0.030	0.070 ± 0.037	34.833 ± 26.179
D	44.000 ± 11.595	71.167 ± 16.293	0.053 ± 0.025	0.165 ± 0.076	11.500 ± 6.986
E	118.000 ± 51.009	102.222 ± 48.815	0.085 ± 0.061	0.170 ± 0.148	*35.556 ± 27.858*
F	88.889 ± 44.895	80.444 ± 41.287	0.056 ± 0.039	0.079 ± 0.049	30.667 ± 32.983

we recommend using a lower-value resin to ensure flexural strength.

The b^* value reflects the measurement along the yellow-blue axis, and the larger the b^* value is, the more yellow the color is [19]. The wavelength of the light emitted by our printer is 405 nm, which represents blue-violet light. As summarized in Table 1, the b^* value of the Group A resin is higher than that of the resins belonging to the other groups, and its mechanical properties are relatively poor in both aspects. This result can possibly be ascribed to the fact that there exists more opaque yellow pigmentation in the resin, which limits the absorption of blue-violet light, thus resulting in poorer mechanical properties. Tahayeri et al. [18] reported that the highest laser intensity was used to print gray resin. This implied that the gray resin absorbed the highest amount of light, which confirmed that it had the best mechanical properties in our experiment.

In addition, Tahayeri et al. [18] reported that the highest and lowest accuracies were achieved when using the white and black resins, respectively. In this study, we did not achieve the highest accuracy when using the white resin but achieved the lowest accuracy when using the black resin. This may be explained by the higher opaque pigmentation of the black resin. Therefore, it is reasonable to assume that the poor printing accuracy achieved when using the black resin may be due to the penetration of light to a depth greater than

Table 5: Relative errors of trueness.

Groups	h_1 (μm)	h_2 (μm)	θ_1 (°)	θ_2 (°)	d (μm)
A	0.0679	0.0595	0.0382	0.0462	0.0109
B	0.0727	0.0631	0.0374	0.0374	0.0125
C	0.0635	0.0550	0.0396	0.0434	0.0124
D	0.0722	0.0656	0.0388	0.0374	0.0131
E	0.0763	0.0650	0.0379	0.0401	0.0096
F	0.0613	0.0542	0.0398	0.0418	0.0111

Table 6: Relative errors of precision.

Groups	h_1 (μm)	h_2 (μm)	θ_1 (°)	θ_2 (°)	d (μm)
A	0.0020	0.0022	0.0068	0.0022	0.0009
B	0.0036	0.0037	0.0051	0.0044	0.0007
C	0.0045	0.0037	0.0035	0.0023	0.0009
D	0.0011	0.0016	0.0033	0.0048	0.0002
E	0.0051	0.0049	0.0053	0.0093	0.0009
F	0.0045	0.0041	0.0035	0.0031	0.0011

the layer thickness corresponding to our setting. Notably, according to the results of a statistical analysis of accuracy (trueness and precision) in this study, a significant difference was found only in the case of the *d* index of the Group E resin. This may be ascribed to the relatively small degree of dispersion of the *d* index, which is reflected in the fact that the value and range of the *d* index along the vertical axis are smaller than those of the other indexes. Moreover, it can be inferred from Tables 5 and 6 that the relative errors of the *d* index are smaller than those of the other indexes. Considering this aspect, the difference between Group E and the other groups in terms of the *d* index is not too large. In addition, in terms of the indexes other than the *d* index, the mean value and dispersion of group E are larger than those of the other groups. Therefore, we believe that the accuracy of the resins with high values is poor. However, the other groups did not exhibit clear maxima and trends in accuracy, and the value range of our study was limited. For this reason, wider value ranges should be studied and discussed in the future.

Interestingly, during the printing process, we found that the printed plate model was thicker than the set value. The height cones of the printed crown-and bridge model were lower than the respective set values. This result may be ascribed to changes in laser intensity during the printing process. When the printer cures thinner layers (thin objects), the metal plate that carries the printed product reflects a greater proportion of the laser light. As the number of cured layers increases (thick object), the reflective effect of the metal plate on the laser decreases.

Although the process of designing and 3D printing dental products is well established and highly individualized, differences in printing parameters and materials used can interfere with the quality of the printed products [20]. In this study, we investigated the influence of photosensitive resin color (value) on the mechanical properties and accuracy of 3D-printed products. We aimed to improve our understanding of the effect of material color on the performance of printed products and provide a color reference for producing clinical dental restorations. However, value accounts for a minor part of the Munsell color system, and more studies must be conducted to explore the Munsell color system in the context of 3D printers. Layer thickness, build direction, angle, intensity, laser speed, curing process, and printing technique are all factors that affect the accuracy of printed models [21]. Aretxabaleta et al. [22] stated that the highest fidelity and accuracy can be achieved with the shortest production time when the printer layer thickness is set to 100 μm. Meanwhile, Alshamrani et al. [23] indicated that the 3D printing layer thickness of 100 μm led to higher flexural strength than those achieved with the layer thicknesses of 25 μm and 50 μm. These results illustrate the need for optimizing the printing parameters. For this reason, we will explore the settings of other parameters in the future.

During the preparation of the plate models, we added support to the 3D-printed samples to satisfy the thickness requirement. When we removed these supports, we attempted to ensure that the models were not stressed. However, some stress may have been induced in them, which would affect their mechanical properties. Another limitation of our study is the print angle. The construction angle of the 3D-printed models in this study was 0°. Osman et al. [24] achieved the best accuracy with the build angle of 135° in their study of the accuracy of 3D printing build orientation on the size of the restoration under DLP processing. Therefore, future studies may consider investigating the effect of value when evaluating the effect of different construction angles.

5. Conclusion

Based on the results of this study, the following conclusions were drawn:

(1) The value of a resin affects the mechanical properties and accuracy of the 3D-printed products.

(2) It is better to secure flexural strength using a lower-value resin.

(3) High-value resins have relatively low accuracy.

Data Availability

The data used to support the findings of this study are included in this article.

Conflicts of Interest

The authors declare that they have no financial or personal relationships with other people or organizations that can inappropriately influence our work.

Authors' Contributions

Jianping Huang and Liming Yu were responsible for the conceptualization; Guihua Ye contributed to the methodology; Qing Lan conducted the validation; Wanxiang Ye and Qi Jia conducted the formal analysis; Kelun Li and Heng Bo Jiang were responsible for data curation; Jianping Huang, Wanxiang Ye, and Jiawen Kong wrote and prepared the original draft; Heng Bo Jiang, Jianping Huang, and Liming Yu wrote, reviewed, and edited the article. All authors have read and agreed to the published version of the manuscript.

Acknowledgments

This article was supported by the Natural Science Foundation of Guangdong Science and Technology Department (2019A1515110724); Guangdong Medical Science and Technology Fund (A2020151); Guangdong Traditional Chinese Medicine Bureau Fund (20222102); Science and Technology Fund of Dongguan (20211800906063); and "Clinical medicine plus" Science and Technology Collaboration Platform and Project of the Affiliated Hospital of Guangdong Medical University (CLP2021B012).

References

[1] G. Oberoi, S. M Nitsch, K Janjić, and A. S. H. Müller, "3D printing-encompassing the facets of dentistry," *Frontiers in Bioengineering and Biotechnology*, vol. 6, p. 172, 2018.

[2] P. Vasamsetty, T. Pss, D. Kukkala, M. Singamshetty, and S. Gajula, "3D printing in dentistry - e," *Materials Today Proceedings*, vol. 26, pp. 838–841, 2020.

[3] R. Ranjan, D. Kumar, M. Kundu, and S. Chandra Moi, "A critical review on Classification of materials used in 3D printing process," *Materials Today Proceedings*, vol. 61, pp. 43–49, 2022.

[4] D. Khorsandi and A. P. S. S. M. S. A. A. A. F. A. R. M. B. V. F. R. P. Fahimipour, "3D and 4D printing in dentistry and maxillofacial surgery: printing techniques, materials, and applications," *Acta Biomaterialia*, vol. 122, pp. 26–49, 2021.

[5] W. Moon and S. B.-S. Y.-S. R. J.-Y. S. H. Kim, "Dimensional accuracy evaluation of temporary dental restorations with different 3D printing systems," *Materials*, vol. 14, no. 6, p. 1487, 2021.

[6] J. Schweiger, D. Edelhoff, and J.-F. Güth, "3D printing in digital prosthetic dentistry: an overview of recent developments in additive manufacturing," *Journal of Clinical Medicine*, vol. 10, no. 9, p. 2010, 2021.

[7] A. Bagheri and J. Jin, "Photopolymerization in 3D printing," *ACS Applied Polymer Materials*, vol. 1, no. 4, pp. 593–611, 2019.

[8] J. F. Besegato, E. I. A. C. R. V Jussiani, and F. M. B. L. S. C. C. M. G. Salomão, "Effect of light-curing protocols on the mechanical behavior of bulk-fill resin composites," *Journal of the Mechanical Behavior of Biomedical Materials*, vol. 90, pp. 381–387, 2019.

[9] E.-H. Lee, J.-S. Ahn, Y.-J. Lim, H.-B. Kwon, and M.-J. Kim, "Effect of layer thickness and printing orientation on the color stability and stainability of a 3D-printed resin material," *The Journal of Prosthetic Dentistry*, 2022.

[10] S. Cochrane, "The Munsell Color System: a scientific compromise from the world of art," *Studies In History and Philosophy of Science Part A*, vol. 47, pp. 26–41, 2014.

[11] J. Liu, H. Su, W. Hu, L. Zhang, and D. Tao, "A minimal Munsell value error based laser printer model," *Neurocomputing*, vol. 204, pp. 231–239, 2016.

[12] J.-Y. Chang and W.-C. T.-K. J.-C. P.-S. J.-H. C.-C. Chen, "Evaluating the accuracy of tooth color measurement by combining the Munsell color system and dental colorimeter," *The Kaohsiung Journal of Medical Sciences*, vol. 28, no. 9, pp. 490–494, 2012.

[13] B. Henriques and M. J. C. M. R. M. D. F. S. Gasik, "Mechanical and thermal properties of hot pressed CoCrMo-porcelain composites developed for prosthetic dentistry," *Journal of the Mechanical Behavior of Biomedical Materials*, vol. 30, pp. 103–110, 2014.

[14] International Standard (Iso), *4660 - Rubber, Raw Natural — Colour index Test*, International Organization for Standardization, Geneva, Switzerland, 2020.

[15] International Standard (Iso), - *Dentistry — Base Polymers —Part 1: Denture Base Polymers*, International Organization for Standardization, Geneva, Switzerland, 20795-1.

[16] International Standard (Iso) 12836, *Dentistry —Digitizing Devices for CAD/CAM Systems for Indirect Dental Restorations— Test Methods for Assessing Accuracy*, International Organization for Standardization, Geneva, Switzerland, 2015.

[17] S. H. Uhm, J. H. Kim, H. B. Jiang et al., "Evaluation of the accuracy and precision of four intraoral scanners with 70% reduced inlay and four-unit bridge models of international standard," *Dental Materials Journal*, vol. 36, no. 1, pp. 27–34, 2017.

[18] A. Tahayeri and M. A. P. D. A. C. S. J. L. L. E. Morgan, "3D printed versus conventionally cured provisional crown and bridge dental materials," *Dental Materials*, vol. 34, no. 2, pp. 192–200, 2018.

[19] Chap 3, *Phillips Science of Dental Materials*, Elsevier Health Sciences, Amsterdam, Netherlands.

[20] W. Piedra-Cascón, V. R. Krishnamurthy, W. Att, and M. Revilla-León, "3D printing parameters, supporting structures, slicing, and post-processing procedures of vat-polymerization additive manufacturing technologies: a narrative review," *Journal of Dentistry*, vol. 109, Article ID 103630, 2021.

[21] F. Emir, G. Ceylan, and S. Ayyıldız, "In vitro accuracies of 3D printed models manufactured by two different printing technologies," *European Oral Research*, vol. 55, no. 2, pp. 80–85, 2021.

[22] M. Aretxabaleta, A. Unkovskiy, B. Koos, S. Spintzyk, and A. B. Xepapadeas, "Accuracy evaluation of additively and subtractively fabricated palatal plate orthodontic appliances for newborns and infants-an in vitro study," *Materials*, vol. 23, no. 15, p. 4103, 2021.

[23] A. A. Alshamrani, R. Raju, and A. Ellakwa, "Effect of printing layer thickness and postprinting conditions on the flexural strength and hardness of a 3D-printed resin," *BioMed Research International*, vol. 2022, Article ID 8353137, 9 pages, 2022.

[24] R. Osman, N. Alharbi, and D. Wismeijer, "Build angle: does it influence the accuracy of 3D-printed dental restorations using digital light-processing Technology?" *The International Journal of Prosthodontics*, vol. 30, no. 2, pp. 182–188, 2017.